Dynamics of Atmospheres and Oceans xxx (2008) xxx–xxx

Contents lists available at ScienceDirect

Dynamics of Atmospheres and Oceans

journal homepage: www.elsevier.com/locate/dynatmoce

Assessment of global numerical models in the East Pacific as evidenced from EPIC2001 project

Julio C. Marín [a,*], G.B. Raga [a], David J. Raymond [b]

[a] Centro de Ciencias de la Atmósfera, Av. Universidad #3000, CP 04510, UNAM, Mexico City, Mexico
[b] Physics Department, New Mexico Tech, 801 Leroy Place, Socorro, NM 87801, USA

ARTICLE INFO

Article history:
Received 19 April 2008
Received in revised form 3 October 2008
Accepted 3 October 2008
Available online xxx

Keywords:
Reanalysis
Analysis
Ocean–atmosphere system
Dropsonde
Buoy mooring systems
Instrument platforms
EPIC2001
East Pacific

ABSTRACT

ERA-40 and NCEP-DOE global Reanalysis and the global tropospheric FNL analysis are compared with observations from the EPIC2001 experiment and data from TAO moorings along 95°W, to assess how they represent the atmospheric conditions in the East Pacific.

All analyses represent reasonably well the mean vertical wind profiles in the atmospheric boundary layer (ABL) and at all heights within the Intertropical Convergence Zone (ITCZ) at 95°W. However, mean vertical zonal wind profiles show a poor agreement in the layer 850–600 hPa from the equator to 5°N. This could cause differences in reproducing the surface meridional pressure gradient, as a result of geostrophic dynamics (Raymond, Bretherton, Molinari, 2006. Dynamics of the Intertropical Convergence Zone of the East Pacific. J. Atmos. Sci. 63, 582–597), that drives the meridional flow into the ITCZ. θ_e vertical profiles, surface fluxes and near-surface temperature present appreciable differences with observations between the equator and 5°N, suggesting that these global analyses must be used with caution in that region.

Analyses seem to represent fairly well the time evolution of the surface meridional wind in the ITCZ and also the transitions of the zonal winds at 850 hPa, as a result of the easterly wave passages over the region. Westerly periods in the ITCZ are associated with strong surface southerly winds, which result in enhanced convection and indicate an increase in the relative circulation of the region. In addition, easterlies coincide with a decrease in relative circulation, which could be related to the decrease in the convective activity. The averaged wind field in the ITCZ is reasonably well

* Corresponding author. Tel.: +52 55 5622 4067/4248; fax: +52 55 5622 4396.
E-mail addresses: juliocma@atmosfera.unam.mx (J.C. Marín), raga@servidor.unam.mx (G.B. Raga), raymond@kestrel.nmt.edu (D.J. Raymond).

0377-0265/$ – see front matter
doi:10.1016/j.dynatmoce.2008.10.001

reproduced by all datasets, supporting their use in dynamical studies in the region. Unfortunately, the same cannot be said for the relative circulation and detrained mass flux since they show large differences with observations.
In general, all analyses could be used to study mean conditions over the study region, taking into account the described limitations.

1. Introduction

Several numerical weather prediction (NWP) centers produce global tropospheric analyses that represent the initial state of the atmosphere for use in forecast models. They are generated from a previous forecast (first guess) of present atmospheric conditions, and are adjusted through data assimilation systems to observations collected from several observational platforms around the world. The use of operational analyses in a specific study may be limited by difficulties in the quality control of assimilated data, scarcity of data over the region of interest and poor representation of the physical processes, combined with problems that may arise due to changes in the NWP model, the analysis and data assimilation techniques, which may interrupt the temporal consistency of the analyzed fields.

In recent years, several reanalysis projects (NCEP-NCAR, NCEP-DOE, ERA-15, ERA-40) were conducted as a cooperative effort among institutions. The main goal of a reanalysis is to produce new atmospheric analyses for a specific period using an improved data assimilation technique and quality control, more observations and keeping the data assimilation-model forecast system unchanged during the project.

The tropics are characterized by a shortage of observations and for this reason, reanalyses have proven to be useful for its study. Many studies that investigate the physical mechanisms driving the atmospheric—oceanic conditions over the tropical Pacific have used reanalysis data as the main dataset or to complement observations (Nigam et al., 2000; Carr and Bretherton, 2001; Stevens et al., 2002; Bretherton et al., 2004a, b; McGauley et al., 2004; Back and Bretherton, 2006; Raymond et al., 2006; Romero-Centeno et al., 2007).

In this paper, ERA-40 and NCEP-DOE global Reanalysis and the global tropospheric FNL analysis are compared with observations to assess how they represent the atmospheric conditions in the East Pacific. Observations come from the East Pacific Investigation of Climate (EPIC2001) experiment, which provides a unique representation of the atmosphere in that region during September–October 2001. Observations from specific Tropical Atmosphere Ocean (TAO) moorings in the East Pacific are also used to complement the comparison. In Section 2, the methodology followed in the study and a description of the different datasets employed are presented. Section 3 shows the results from comparisons and finally, Section 4 presents the conclusions of the study.

2. Data and methodology

Observations from buoys and aircraft during the East Pacific Investigation of Climate 2001 (EPIC2001) field experiment provide the observational evidence to assess the performance of global analyses in the East Pacific region. The representation of the atmospheric vertical structure in global assimilated data was analyzed along the 95° W longitude using vertical profiles of equivalent potential temperature (following Bolton, 1980), and the zonal and meridional components of the wind. Saturation fraction was also used as a measure of the moisture content in a specific layer of the atmosphere. The study of near-surface variables along 95° W included the analysis of temperature, relative humidity, both wind components and surface fluxes (wind stress, sensible and latent heat) calculated from the Coupled Ocean Atmosphere Response Experiment (COARE) v.3.0a bulk-flux algorithm.

The investigation of the atmospheric conditions in the Intertropical Convergence Zone (ITCZ) during the EPIC2001 period was performed in a 4° × 4° region centered at 10°N, 95° W (EPIC domain). It included the analysis of the wind, the detrained mass flux and the relative circulation over that

Please cite this article in press as: Marín, J.C., et al., Assessment of global numerical models in the East Pacific as evidenced from EPIC2001 project. Dyn. Atmos. Oceans (2008), doi:10.1016/j.dynatmoce.2008.10.001

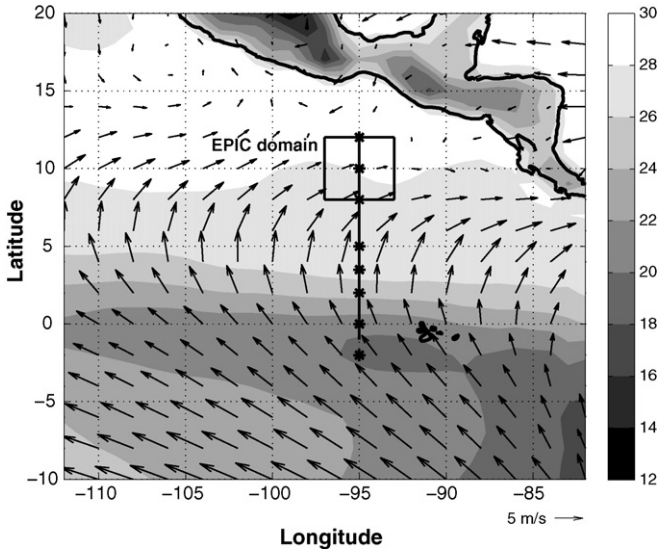

Fig. 1. Map showing the EPIC domain in the East Pacific, the C-130 transect and the TAO mooring array (stars) along 95°W. Vectors and shading show the mean near-surface winds and surface temperature (over sea or land) from FNL for September–October 2001. Vectors were plotted every 2°.

region. All comparisons in this study were made using the nearest time in assimilated data to observations.

2.1. EPIC2001 project

The EPIC2001 field experiment was carried out during September–October 2001 in the East Pacific region (Raymond et al., 2004; Bretherton et al., 2004b). Among the purposes of the experiment was to reach a better understanding of different physical processes in the region where numerical models present large discrepancies with observations (e.g. deep cumulus convection and atmospheric boundary layer (ABL) dynamics). Fig. 1 shows the region of study where the EPIC domain is indicated by the square and the "stars" indicate the location of TAO buoys along 95°W. Near-surface wind flow and surface temperature from FNL, averaged for September–October 2001, illustrate the advantage of using the assimilated datasets for studies in the region due to the limited spatial and temporal scale of the available observations. A reasonable agreement in reproducing the atmospheric conditions along 95° W could support their use over a much larger area in the East Pacific.

Two research aircraft operated in the East Pacific during the field campaign performing different flight patterns (Raymond et al., 2003). The C-130 aircraft (NSF, operated by NCAR) flew to the equator along the 95° W longitude line (Fig. 1) making in-situ measurements at low altitudes. In its return flight at an altitude of 6300 m, dropsondes were launched from the equator to 12° N every 1°, allowing for a height-latitude cross-section of the atmosphere. The P3 aircraft (NOAA) flew at 1900 m over the EPIC domain in the ITCZ, launching dropsondes every 1°. Dropsonde data from eight missions along the 95°W, and 10 missions over the ITCZ that include the zonal and meridional components of the wind, temperature and humidity variables were used in this study.

2.2. TAO buoy array

The Tropical Atmosphere Ocean (TAO) moorings (McPhaden et al., 1998) provide data at different sampling times for climate research. Data from the moorings at 0, 2°N, 3.5°N, 5°N, 8°N, 10° N and 12° N located along the 95° W longitude (Fig. 1) were obtained from

Please cite this article in press as: Marín, J.C., et al., Assessment of global numerical models in the East Pacific as evidenced from EPIC2001 project. Dyn. Atmos. Oceans (2008), doi:10.1016/j.dynatmoce.2008.10.001

http://www.pmel.noaa.gov/tao/data_deliv/for the EPIC2001 period (September–October 2001). They included observations of sea surface temperature (SST), near-surface air temperature, wind and relative humidity, sea level pressure (SLP), longwave and shortwave radiation fluxes. TAO buoys at the equator and 2° N measured data only from early October for the period of the EPIC2001 experiment. The type of sensors used on TAO moorings, their resolution, measurement ranges, and the height at which measurements are made can be found at http://www.pmel.noaa.gov/tao/proj_over/sensors.shtml.

The COARE v.3.0a bulk flux algorithm (Fairall et al., 2003) was used to calculate bulk wind stress, sensible and latent heat fluxes from surface variables. The cool skin parameterization was used to calculate skin SST from SST measurements at 1 m depth from TAO buoys. The COARE algorithm calculates surface fluxes using the wind relative to the interface. Surface currents were not available at all TAO buoys for the whole period of study and none of the assimilated data include this variable. For this reason, the surface current was set to 0 in the bulk flux calculations.

Bulk sensible and latent heat fluxes and surface stress obtained from the COARE v.3.0a bulk flux algorithm were calculated for TAO observations and for reanalysis and FNL at 18 UTC. Data were averaged for the eight missions. De Szoeke et al. (2005a) compared bulk sensible and latent heat fluxes (calculated with the COARE algorithm) from TAO data with fluxes from C-130 in situ data calculated with the bulk and the eddy correlation method. They found comparable mean biases between TAO fluxes and fluxes calculated from C-130 in situ data using daily TAO data for September–October 2001 or using TAO data for the hours of the C-130 flights. The C-130 eddy correlation sensible heat flux showed good agreement with bulk fluxes calculated from C-130 and TAO data at all latitudes except at 5°N, which they attributed to a 2 K warm bias observed in TAO data at that latitude. Appreciable differences in the latent heat flux were only observed at 2°N, 3. 5° N and 5° N where bulk fluxes from TAO were 0–50 W/m^2 lower than bulk and eddy correlation C-130 fluxes. SST from FNL was used to calculate ERA40 fluxes, and precipitation rate and radiative fluxes from NCEP-DOE Reanalysis 2 were used to calculate FNL fluxes since none of these data were available for ERA40 and FNL. TAO fluxes at 8° N were not calculated since no wind measurements were recorded over the EPIC period at that latitude. Latent heat flux from TAO at the equator was not calculated since no humidity was available for that period.

2.3. Global datasets

2.3.1. FNL tropospheric analyses

FNL is the Final run of GDAS, which is the Global Data Assimilation System of the Global Forecast System (GFS) model, run four times per day (00, 06, 12, and 18 UTC) at the National Centers for Environmental Prediction (NCEP). FNL data for the period of study was obtained from http://www.dss.ucar.edu/datasets/ds083.2/data. It includes variables at the surface and 26 vertical pressure levels from 1000 to 10 hPa at a horizontal resolution of $1° \times 1°$ every 6 h.

2.3.2. NCEP/DOE Reanalysis project

NCEP-DOE Reanalysis 2 (Kanamitsu et al., 2002) is an improved version of the NCEP Reanalysis 1 model that fixed errors and updated parameterizations of physical processes. Data for this reanalysis was provided by the NOAA/OAR/ESRL PSD, Boulder, Colorado, USA, from http://www.cdc.noaa.gov/. Data is available at 00, 06, 12 and 18 UTC, at a horizontal resolution of $2.5° \times 2.5°$ and 12 pressure levels from 1000 to 100 hPa. Surface variables are available in a global Gaussian lat/lon grid and they were interpolated to the longitudes and latitudes of interest to compare with surface observations. The reanalysis will be referred to as NDR2 in the rest of the paper.

2.3.3. ECMWF 40 Year reanalysis (ERA-40)

The ERA-40 Reanalysis data (hereafter referred to as ERA40) is available four times per day at 00, 06, 12 and 18 UTC in a global grid, with $2.5° \times 2.5°$ of horizontal resolution, for the period from mid-1957 to 2002 (Uppala et al., 2005). Variables at 13 pressure levels from 1000 to 100 hPa and at the surface were obtained for the EPIC period from the ECMWF data server at http://data.ecmwf.int/data/d/era40_daily.

Please cite this article in press as: Marín, J.C., et al., Assessment of global numerical models in the East Pacific as evidenced from EPIC2001 project. Dyn. Atmos. Oceans (2008), doi:10.1016/j.dynatmoce.2008.10.001

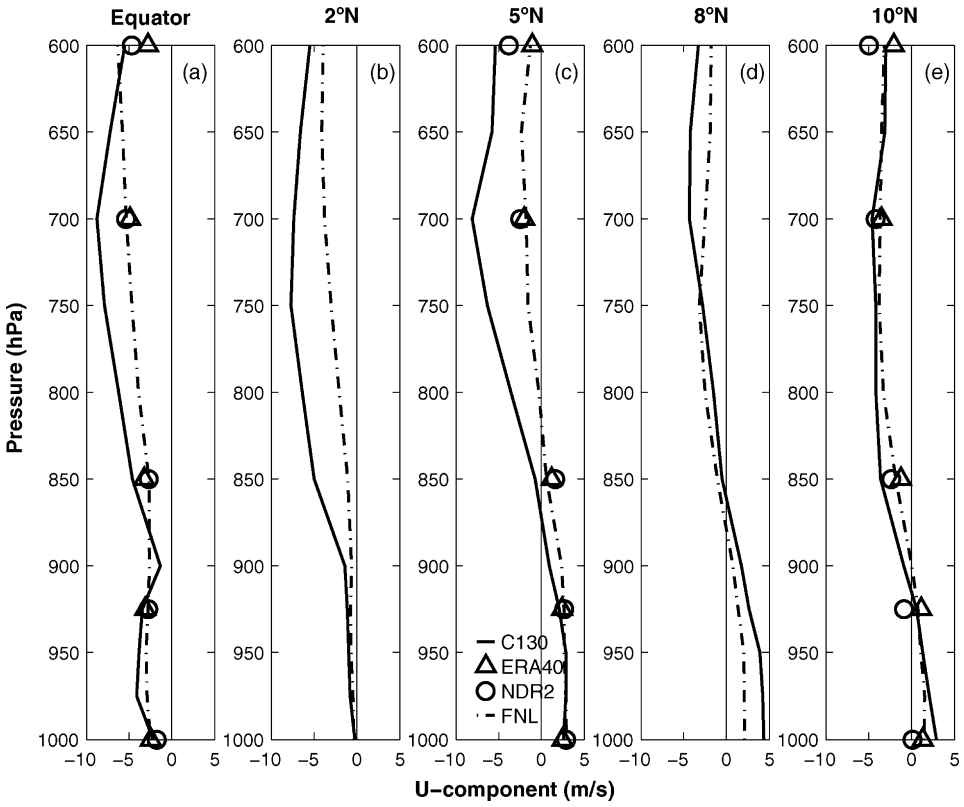

Fig. 2. Vertical profiles of the zonal wind averaged over the eight C-130 missions at (a) the equator, (b) 2°N, (c) 5°N, (d) 8° N and (e) 10° N for dropsonde observations (solid line), ERA40 (triangles), NDR2 (circles) and FNL (dash-dotted line).

3. Results

3.1. Mean conditions along 95°W

This section presents the comparison between observations and the three global datasets averaged for the eight missions along the 95° W longitude during September and October 2001.

3.1.1. Mean vertical wind structure

Fig. 2 a, c and e show the vertical profiles of the zonal wind from dropsondes, NDR2, ERA40 and FNL at the equator, 5° N and 10°N, respectively. Vertical profiles from dropsondes and FNL are also shown in Figs. 2 b and d for latitudes 2° N and 8° N due to the higher horizontal resolution of this data. The comparison with reanalysis is made at five pressure levels (1000, 925, 850, 700 and 600 hPa), while that with FNL uses 11 pressure levels (1000, 975, 950, 925, 900, 850, 800, 750, 700, 650 and 600 hPa).

The three datasets are very similar from 1000 to 700 hPa. The largest differences among them are observed at 600 hPa at all latitudes. The best agreement with observations is generally shown in the ABL (1000–900 hPa layer) from the equator to 7°N. The largest differences with observations are also shown over these latitudes since none of the assimilated datasets reproduce accurately the predominant easterly winds present in the layer 850–600 hPa (Figs. 3a and 4a).

Observations at 1000, 925, 850, 700 and 600 hPa and at the equator, 5° N and 10° N were compared with analyses using scatter plots in order to investigate whether analyses correctly represent the

Please cite this article in press as: Marín, J.C., et al., Assessment of global numerical models in the East Pacific as evidenced from EPIC2001 project. Dyn. Atmos. Oceans (2008), doi:10.1016/j.dynatmoce.2008.10.001

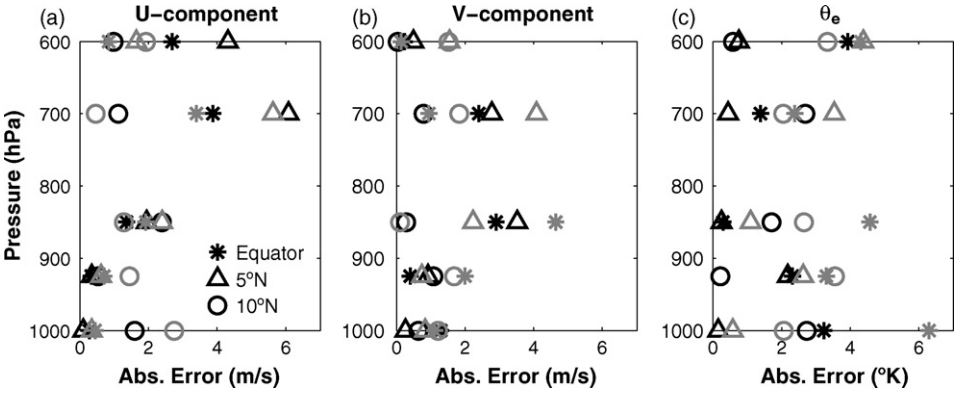

Fig. 3. Vertical profiles of absolute errors between dropsondes and ERA40 (black) and between dropsondes and NDR2 (gray) for (a) the zonal wind, (b) the meridional wind and (c) θ_e at the equator (stars), at 5° N (triangles) and at 10° N (circles).

observed zonal wind behavior during each C-130 mission. Similar results as those mentioned above, showing the least scatter in the ABL at the equator and at 5°N, and the largest scatter in the 850–600 hPa layer, at the same latitudes, were found. Fig. 5 shows only results for 5° N and 10°N, and for pressure levels 925 and 700 hPa. Some panels show fewer than eight datapoints since not all flights were available.

The v-component comparison (Fig. 6) shows a better agreement between observations and assimilated datasets at all pressure levels and latitudes. Strong meridional winds within the ABL are the result of the large surface meridional pressure gradient present in this region as a consequence of the sea surface temperature (SST) front, approximately located at 95° W between 1° S and 4° N (De Szoeke et al., 2005a) during the EPIC2001 experiment. Meridional winds accelerated by this mechanism finally converge into the ITCZ resulting in the observed low values. These East Pacific characteristics have been investigated by Lindzen and Nigam (1987), Yin and Albrecht (2000) and Chelton et al. (2001) and more recently using EPIC2001 observations, by McGauley et al. (2004), De Szoeke et al. (2005a,b) and Raymond et al. (2006).

All assimilated datasets represent reasonably well the strong meridional winds in the ABL from the equator to 7° N and their decrease in strength with height in that layer. However, they are generally underestimated in FNL and overestimated in NDR2 and ERA40. The best agreement between analyses and observations is generally present in the ABL at all latitudes (Figs. 3 b and 4b).

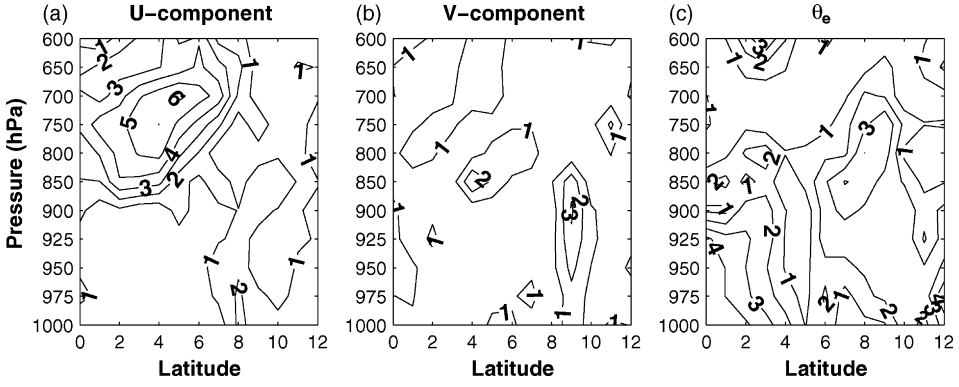

Fig. 4. Pressure-latitude cross-section of absolute errors for FNL. (a) u-Component, (b) v-component of the wind and (c) θ_e. Contour intervals are drawn at 1 ms^{-1} for both wind components and at 1 K for θ_e.

Please cite this article in press as: Marín, J.C., et al., Assessment of global numerical models in the East Pacific as evidenced from EPIC2001 project. Dyn. Atmos. Oceans (2008), doi:10.1016/j.dynatmoce.2008.10.001

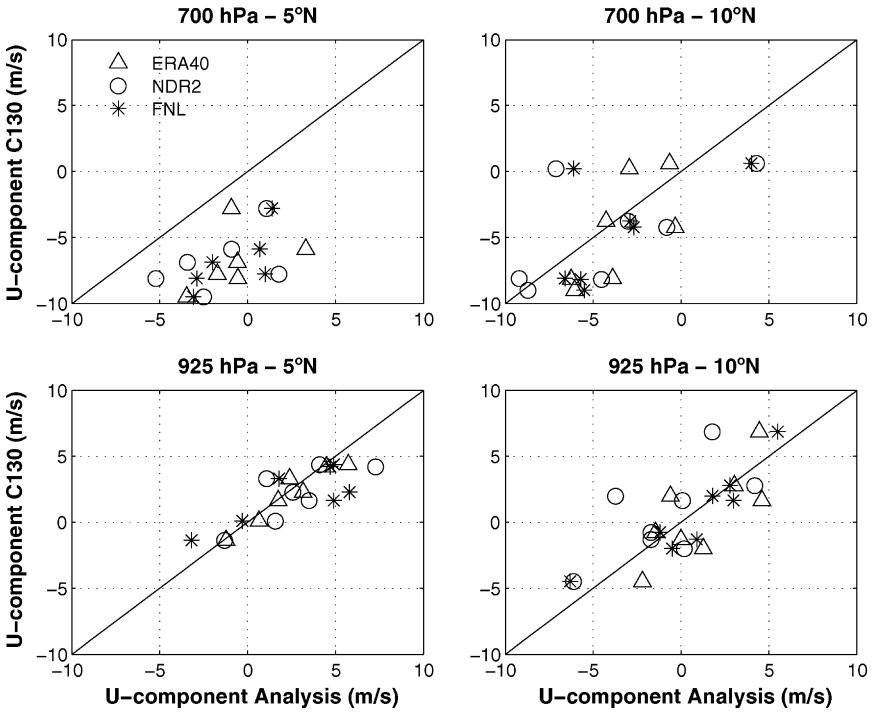

Fig. 5. Scatter plots of zonal winds from dropsondes vs ERA40 (triangle), NDR2 (circle) and FNL (star) at 925 hPa and 700 hPa, and at 5° N (first column) and 10° N (second column).

NDR2 and FNL reproduce the shallow meridional cell observed at 5° N (although they underestimate its magnitude), while ERA40 does not (Fig. 6c). This circulation was observed using C-130 dropsondes from EPIC (Zhang et al., 2004) as a northerly flow above the ABL (900–700 hPa), from approximately 10° N to the equator. Scatter plots for the v-component (not shown) also show the same behavior described in the mean vertical profiles analysis.

The previous analysis of both wind components show that the assimilated datasets represent reasonably well the vertical structure of mean winds in the ABL at all the latitudes studied. The meridional component is better represented in analyses than the zonal component. The best agreement is shown in the ABL, from the equator to 7°N, with absolute errors for both components less than 1.3, 2.0 and 1.6 ms^{-1} in ERA40, NDR2 and FNL, respectively. At these latitudes, but above the ABL, the zonal wind behavior is poorly captured by datasets. Within the EPIC domain the agreement of the ABL winds is worse in the analyses than at the southernmost latitudes, while at higher levels, the agreement improves.

3.1.2. Mean vertical temperature structure

At the equator and 2°N, the ABL is predominantly well mixed from 1000 hPa up to 925 and 900 hPa, respectively (Fig. 7). All datasets overestimate θ_e in the ABL at these latitudes and ERA40 shows the smallest absolute errors (Figs. 3 c and 4c). On the other hand, the ABL is predominantly unstable from 5° N to 10° N and θ_e is in general underestimated by all datasets. Above the ABL, FNL and ERA40 show a much better agreement with observations than NDR2 (Figs. 3 c and 4c).

Vertical θ_e lapse rates between layers 925–1000 and 850–925 hPa were calculated for C-130 dropsondes and global datasets (Table 1) to analyze how they represent the stability in the ABL and immediately above, as a function of latitude. A well-mixed layer is observed in the ABL at the equator and 2°N. Only FNL shows a mixed layer at the equator whereas the reanalyses indicate moist unstable conditions. Above the ABL, all assimilated datasets show a weaker inversion layer than observed. Moist

Please cite this article in press as: Marín, J.C., et al., Assessment of global numerical models in the East Pacific as evidenced from EPIC2001 project. Dyn. Atmos. Oceans (2008), doi:10.1016/j.dynatmoce.2008.10.001

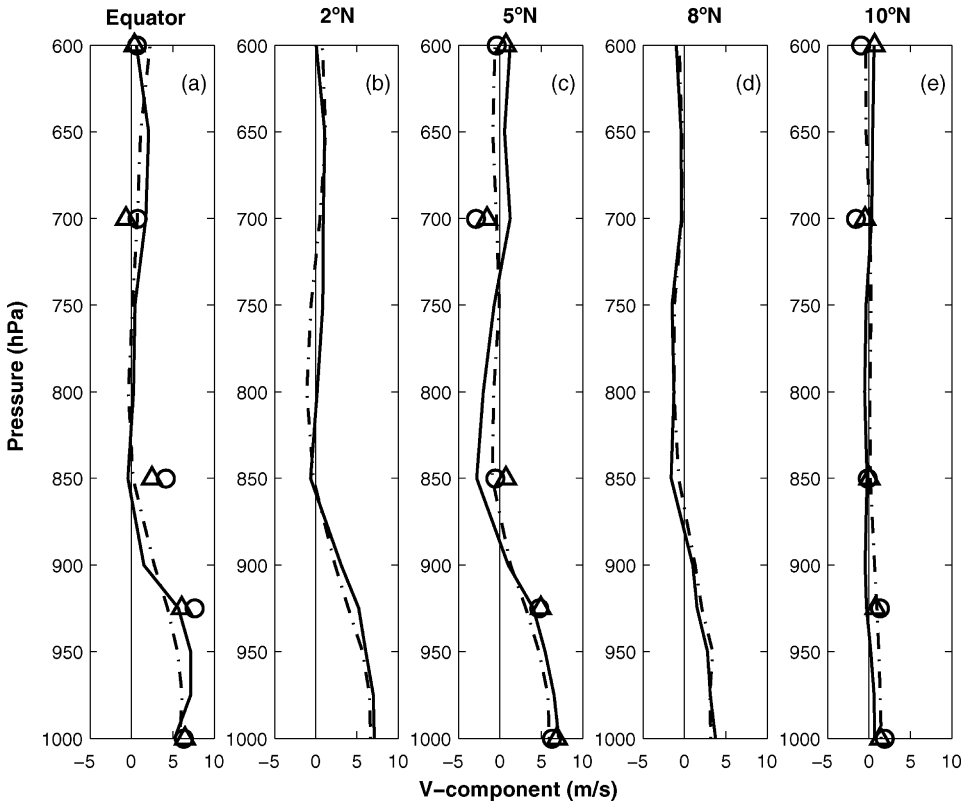

Fig. 6. Same as Fig. 2 but for the v-component.

unstable conditions predominate in observations from 5° N to 10° N in the layer 1000–850 hPa. All analyses reproduce a negative lapse rate in this region, except at 5°N, but FNL shows a much better agreement with observations.

3.1.3. Saturation fraction

The development of deep convection is influenced by atmospheric moisture, specially at mid-levels (Brown and Zhang, 1997). Bretherton et al. (2004a) found a strong relationship between precipitation rate and the saturation fraction (the ratio of precipitable water to saturated precipitable water) in the tropical oceans using satellite observations and reanalysis data. The numerical study of Raymond and Zeng (2005) also suggested a strong dependence of precipitation upon atmospheric relative humidity.

Saturation fraction from observations and assimilated data were compared to analyze how well the global datasets represent the near-saturated atmosphere in the East Pacific region along 95°W. It was

Table 1
Lapse rate (LR) of θ_e (K) in the layers 1000–925 and 925–850 hPa for dropsondes, ERA40, NDR2 and FNL.

LR θ_e (K)	θ_e (925 hPa)– θ_e (1000 hPa)					θ_e (850 hPa)– θ_e (925 hPa)				
	Equator	2°N	5°N	8°N	10°N	Equator	2°N	5°N	8°N	10°N
C-130	−0.33	−0.92	−2.0	−4.14	−6.42	10.5	7.29	−0.85	−2.55	−4.52
ERA40	−1.25	–	−4.34	–	−3.45	7.9	–	1.58	–	−3.03
NDR2	−3.32	–	−4.05	–	−7.9	2.64	–	0.68	–	−3.61
FNL	−0.52	−1.97	−3.36	−5.93	−6.76	4.36	3.66	−1.74	−3.77	−3.56

Please cite this article in press as: Marín, J.C., et al., Assessment of global numerical models in the East Pacific as evidenced from EPIC2001 project. Dyn. Atmos. Oceans (2008), doi:10.1016/j.dynatmoce.2008.10.001

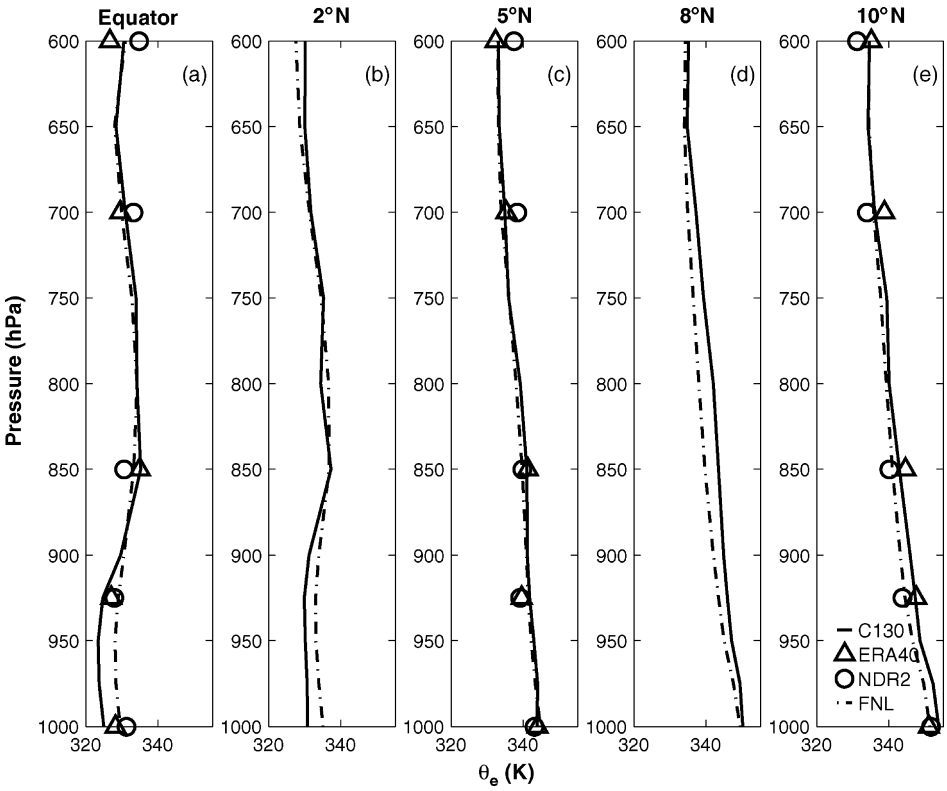

Fig. 7. Same as Fig. 2 but for θ_e.

calculated using the following expression:

$$S_f = \frac{\int_{1000}^{600} q_v \, dp}{\int_{1000}^{600} q_{vs} \, dp} \approx \frac{\sum_{k=1}^{4} (dp_k/2)(q_v(k) + q_v(k+1))}{\sum_{k=1}^{4} (dp_k/2)(q_{vs}(k) + q_{vs}(k+1))} \quad (1)$$

where q_v and q_{vs} are the mixing ratio and saturated mixing ratio of water vapor, respectively.

Saturation fraction values calculated from (1) using dropsondes along 95° W were compared with those calculated from reanalyses and FNL at the equator, 5° N and 10°N (Fig. 8). The integration was made over the layer 1000–600 hPa, using the five pressure levels available in reanalysis. Saturation fraction from FNL was also calculated at those pressure levels for a better comparison among datasets. The least scatter is observed in Fig. 8 c for FNL. The RMSE of the saturation fraction values for all latitudes (Table 2) show the smallest value for FNL. Observed saturation fraction values less than 0.7 are

Table 2
RMSE of saturation fraction between dropsondes and global analyses along the 95°W.

	Equator	5°N	10°N	All
FNL	0.04	0.05	0.08	0.06
ERA40	0.07	0.06	0.14	0.09
NDR2	0.07	0.11	0.06	0.09

Please cite this article in press as: Marín, J.C., et al., Assessment of global numerical models in the East Pacific as evidenced from EPIC2001 project. Dyn. Atmos. Oceans (2008), doi:10.1016/j.dynatmoce.2008.10.001

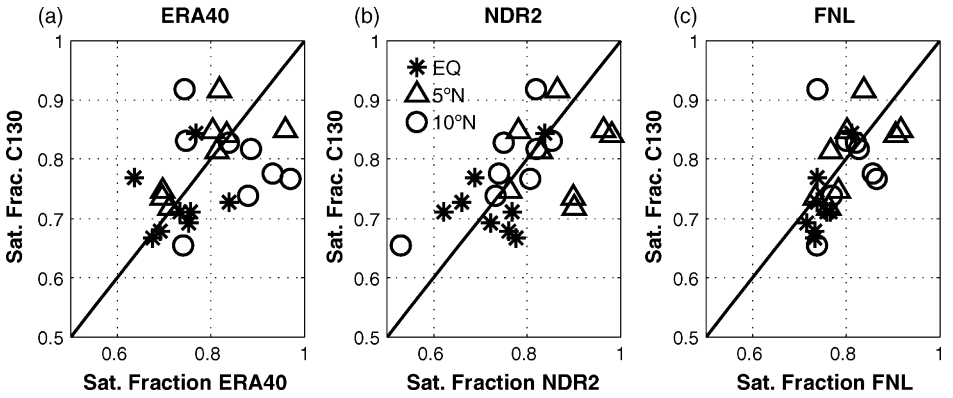

Fig. 8. Scatter plots of saturation fraction from dropsondes vs (a) ERA40, (b) NDR2 and (c) FNL at the equator (stars), 5° N (triangles) and 10° N (circles). The solid line represents the 1:1 relation.

overestimated by the assimilated datasets at all latitudes, while those larger than 0.9 are underestimated (Fig. 8). A drier 1000-600 hPa layer is observed at the equator than at the other latitudes. FNL presents the least scatter at the equator and 5° N and NDR2 shows the best agreement at 10°N.

3.1.4. Mean state at the surface

A correct representation of the surface pressure over this region is very important due to the large surface meridional gradient present as a consequence of the SST front. It causes strong meridional winds to flow from the equator to the ITCZ, which is a forcing mechanism for the development of deep convection in the ITCZ. Mean sea level pressure (MSLP) from analyses were compared with observations at TAO buoys and with surface pressure derived from C-130 in situ data during the 95° W missions (Fig. 9). C-130 pressures were calculated using radar altimeter data, the hydrostatic equation and removing the diurnal cycle of pressure as described by Raymond et al. (2006). MSLP values were averaged for the eight C-130 missions and 12 UTC was chosen from analyses and TAO buoys for a better comparison with C-130 data.

MSLP from C-130 and TAO data differ by less than 0.6 hPa at all latitudes. They both show a decrease with latitude larger than 2.2 hPa from the equator to the ITCZ region. NDR2 represents much better

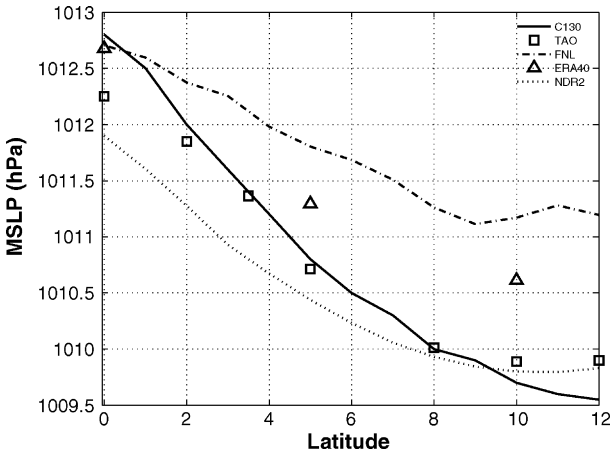

Fig. 9. Latitudinal variation of MSLP along 95° W averaged for all eight C-130 missions for TAO data (squares), C-130 in situ data (solid line), FNL (dash-dotted line), ERA40 (triangle) and NDR2 (dotted line).

Please cite this article in press as: Marín, J.C., et al., Assessment of global numerical models in the East Pacific as evidenced from EPIC2001 project. Dyn. Atmos. Oceans (2008), doi:10.1016/j.dynatmoce.2008.10.001

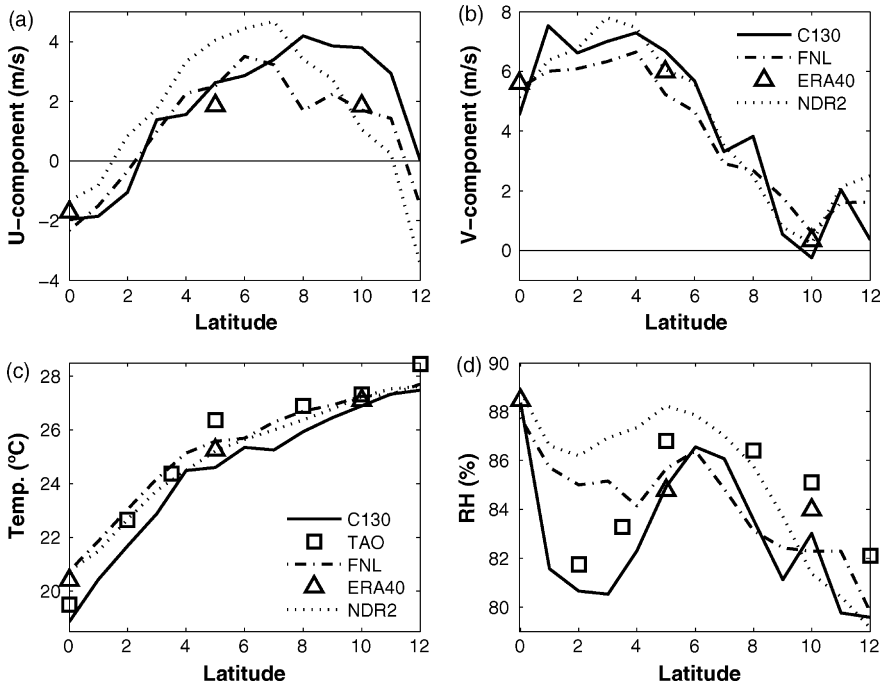

Fig. 10. Latitudinal variation of (a) zonal wind, (b) meridional wind, (c) temperature and (d) relative humidity for C-130 dropsondes (solid line), TAO data (squares), FNL (dash-dotted line), ERA40 (triangle) and NDR2 (dotted line). Wind values correspond to an altitude of 10 m. Temperature and relative humidity values correspond to an altitude of 2 m; except those from TAO, which are measured at 3 m.

the observed behavior of surface pressure with latitude; however it is slightly underestimated south of the ITCZ. Reanalyses differ by less than 1 hPa from observations at all latitudes, and FNL, which presents the least agreement, shows absolute errors less than 1.5 and 2 hPa, compared with TAO and C-130 data, respectively.

Wind components at 10 m from reanalysis and FNL were compared with the closest value in dropsondes to that height within the range 9–15 m, averaged over the eight C-130 missions. Fig. 10 a and Table 3 show that zonal winds from assimilated data present the best agreement with observations from the equator to 7°N. NDR2 shows the largest differences with observations along that longitude. The v-component comparison (Fig. 10b) shows a reasonable good agreement for all datasets, in spite of the MSLP differences with observations shown by FNL and ERA40 in Fig. 9. NDR2 and ERA40 present, in general, the best agreement with observations (Table 3), except a 2 ms^{-1} difference shown by NDR2 at 12°N.

Near-surface air temperature and relative humidity are available at 2 m from analyses, and were compared with the closest values from C-130 dropsondes and with measurements at 3 m from 95° W TAO buoys (Figs. 10 c,d). Fig. 10 c shows the air temperature variation with latitude along the 95°W,

Table 3
Absolute errors between dropsondes and global analyses for wind components at 10 m along the 95°W.

	u-Component (ms^{-1})		v-Component (ms^{-1})	
	South of 7°N	North of 7°N	South of 7°N	North of 7°N
FNL	< 0.7	< 2.5	< 1.5	< 1.3
ERA40	< 0.8	2.0	< 1.1	0.6
NDR2	< 1.9	< 3.5	< 1.2	< 2.1

Please cite this article in press as: Marín, J.C., et al., Assessment of global numerical models in the East Pacific as evidenced from EPIC2001 project. Dyn. Atmos. Oceans (2008), doi:10.1016/j.dynatmoce.2008.10.001

indicating some differences between the two types of observations. TAO data from moorings at the equator and 2° N were only available in early October and only the average for two days is shown. All the other data are averaged over the eigth C-130 missions. All datasets overestimate the 2 m air temperature obtained from C-130 at all latitudes. The least agreement with dropsondes is observed from the equator to 3° N in all datasets and the largest difference is present at the equator. This confirms what was observed when θ_e vertical profiles were analyzed, that assimilated data do not represent accurately the ABL air temperature over the cold tongue region. At the equator, comparison with dropsondes shows absolute errors of 1.5 ° C for ERA40 and 1.9 ° C for NDR2 and FNL. Absolute errors decrease with increasing latitude and values less than 0.5 ° C are observed over the ITCZ in all analyses.

Fig. 10 c also shows the comparison with TAO data at the equator, 2°N, 5°N, 8°N, 10° N and 12°N. At the equator, 2°N, 8° N and 10° N all analyses show a better or similar agreement with TAO than with dropsondes. On the other hand, at 5° N and 12°N, larger differences with TAO are observed than with dropsondes in all datasets. This could be related with the fact that TAO observations are included in NCEP datasets for the EPIC period. TAO observations do not seem to be included in ERA-40, but it shows a similar agreement with observations as that shown by the other datasets. Abarca (2005) compared temperature, winds and relative humidity from TAO buoys at 95° W with in situ measurements from C-130 at the latitudes it flew over the buoys. Air temperatures from C-130 were always smaller than those measured by TAO sensors, which coincides with that shown in this study using dropsonde data. Relative humidity also showed discrepancies between both measurement platforms. Differences between TAO data and dropsondes could be related with the fact that buoys from TAO are moored at fixed latitudes and longitudes and measurements from dropsondes were sometimes made several km away from 95° W or from the latitudes of interest. The poorest representation of the near-surface temperature is observed at the equator in all global datasets with absolute errors as large as 1.9 °C. At 5°N, TAO shows a larger temperature value than that observed in dropsondes and that shown in analyses. As mentioned in Section 2, De Szoeke et al. (2005a) attributed it to a 2 K warm bias in the TAO mooring at that latitude.

Relative humidity values from TAO are larger than those from dropsondes at all latitudes but they show the same variation with latitude (Fig. 10d). All analyses show a good agreement with observations. The largest differences (6.4% and 4.6%) are shown in NDR2 and FNL from 1° N to 4°N; however, they are small and do not introduce large errors.

Bulk sensible and latent heat fluxes and surface stress obtained from the COARE v.3.0a bulk flux algorithm are presented in Fig. 11. Sensible and latent heat fluxes increase from the equator to a peak between 2– 3° N where the maximum air temperature–SST difference is observed and they decrease with increasing latitude, with minimum values over the ITCZ. Fluxes from analyses show this latitudinal variation, although some differences are present among them. Larger differences in heat fluxes among global datasets are observed from 2° N to 7°N. At 5° N and 12° N sensible and latent heat fluxes are overestimated by analyses.

Wind stress shows the maximum value from 3° N to 5° N where peak near-surface meridional winds were observed (Figs. 2 c and 10b). They decrease with latitude showing minimum values over the ITCZ, due to the small near-surface wind values in that region as a result of convergence. All analyses reproduce this latitudinal dependence. Stresses are overestimated in all analyses at the equator and 2° N and they are underestimated at 10 and 12°N. Larger differences are also observed between 2° N and 7°N.

The analysis of near-surface variables and surface fluxes presented here, indicates that results from these global analyses must be used with caution, specifically in the region between the equator and 5°N, where the largest differences with observations are shown.

3.2. The ITCZ EPIC domain

Dropsondes launched in the EPIC domain by the P3 and the C-130 aircraft were used to obtain time series of wind components averaged over that region at several levels. A quantitative comparison with reanalysis and FNL cannot be made due to the different horizontal resolution of datasets and the averaging region. However, a qualitative comparison can indeed be made to investigate how analyses reproduce the time evolution of the ITCZ environment.

Please cite this article in press as: Marín, J.C., et al., Assessment of global numerical models in the East Pacific as evidenced from EPIC2001 project. Dyn. Atmos. Oceans (2008), doi:10.1016/j.dynatmoce.2008.10.001

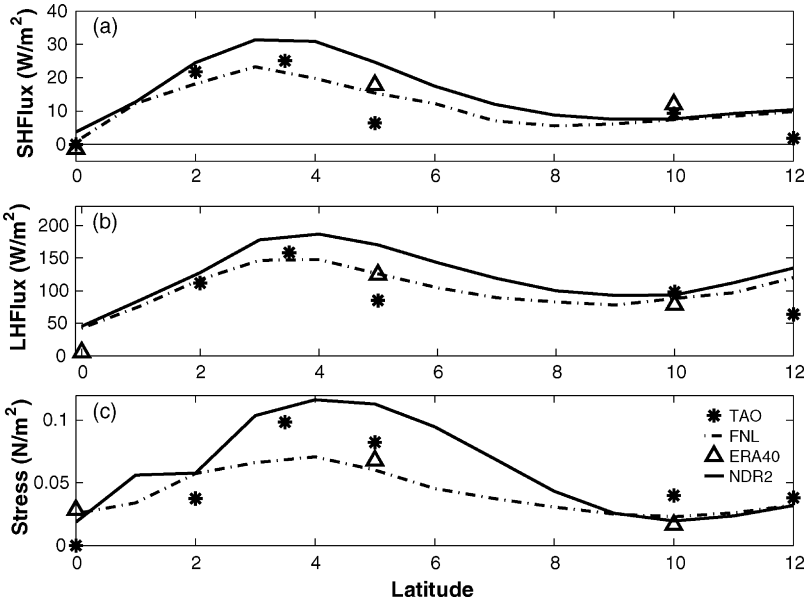

Fig. 11. Bulk fluxes variation with latitude along 95° W for TAO observations (black stars), ERA40 (triangles), FNL (dash-dotted line) and NDR2 (solid line). (a) Sensible heat flux, (b) latent heat flux and (c) wind stress. Fluxes are averaged for all eight C-130 missions.

Fig. 12 a shows the time evolution of the u-component of the wind at 850 hPa. Variations from easterly to westerly wind and vice-versa are associated with the passage of easterly waves over the EPIC area (Petersen et al., 2003) that later developed into tropical cyclones (named in the figure). All analyses represent very well the transition from westerlies on 29 September to easterlies on 2 October and its persistence in October. However, large differences exist among datasets. FNL and ERA40 show the best agreement representing the changes in wind direction. NDR2 does not represent very well the period from 14 to 28 September 2001. In general, all analyses seem to overestimate the u-component. Westerly episodes in the layer 810–830 hPa were correlated with enhanced deep convection in this region and strong ABL southerly winds as a result of geostrophic dynamics (Raymond et al., 2006).

The time evolution of meridional surface winds (Fig. 12b) averaged over the EPIC domain shows that all analyses reproduce reasonably well the peaks in this variable associated with westerlies above the ABL. The largest differences with observations from 5 to 10 October are observed in FNL, despite the fact that it presents the best agreement in this period in the zonal winds aloft. On 23 September the strongest surface meridional wind is observed, but easterlies dominate at 850 hPa as a result of deep convective activity in the region that produced large surface rainfall rates for several hours (Zuidema et al., 2006). Above that height, westerlies dominate and the correlation between westerlies above the ABL and enhanced surface meridional winds is better observed.

The relative circulation and the detrained mass flux over the EPIC domain were calculated at each pressure level from dropsondes launched on 10 missions with the P3 aircraft and from reanalysis and FNL data. A qualitative comparison between observations and analyses was made to study how they represent these variables at each level in the EPIC region. The following expressions:

$$\Gamma = \int_A \left(\frac{\partial v}{\partial x} - \frac{\partial u}{\partial y} \right) \mathrm{d}A \tag{2}$$

$$\Delta = \int_A \left(\frac{\partial u}{\partial x} + \frac{\partial v}{\partial y} \right) \mathrm{d}A \tag{3}$$

Please cite this article in press as: Marín, J.C., et al., Assessment of global numerical models in the East Pacific as evidenced from EPIC2001 project. Dyn. Atmos. Oceans (2008), doi:10.1016/j.dynatmoce.2008.10.001

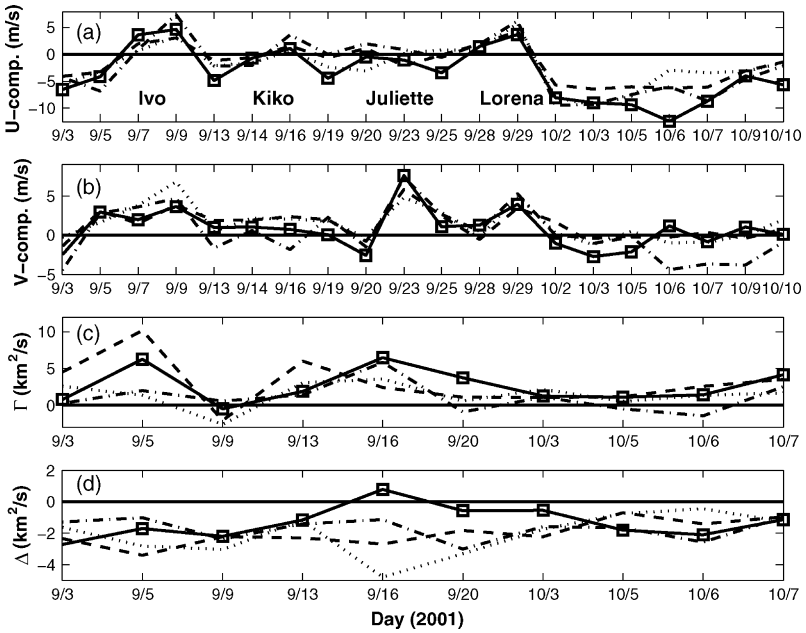

Fig. 12. Time evolution of (a) zonal wind at 850 hPa, (b) meridional wind at the surface, (c and d) relative circulation and detrained mass flux averaged over the layer 1000–850 hPa for dropsondes (squares), FNL (dash-dotted line), ERA40 (dashed line) and NDR2 (dotted line). Values are averaged over the EPIC domain.

were used to calculate the relative circulation (Γ) and the detrained mass flux (Δ), where A represents the integration area, dA is an area element and u and v are the wind components.

Fig. 12 c shows the relative circulation of the EPIC region averaged over the 1000–850 hPa layer for observations and assimilated data. P3 dropsondes show two peaks in relative circulation and then a period of small relative circulation values from 3 to 7 October. The first peak from 3 to 9 September coincides with the transition from easterlies to westerlies at 850 hPa and enhanced surface meridional winds as a result of the passage of an easterly wave that later gave rise to tropical storm Ivo. Another increase in relative circulation is observed later from 13 to 16 September. Zonal winds also transition from easterlies to westerlies over that period and surface northerly winds predominate although they are not too strong. The decrease in relative circulation observed from 3 October coincides with the days when easterlies dominate and a decrease in deep convection was observed in the EPIC domain (Raymond et al., 2006). Surface meridional winds are also weak southerly or even northerly in this period. The analysis of this figure indicates that the relative circulation in the ITCZ region increases when periods of westerlies above the ABL and strong surface southerly winds are observed. All analyses show two peaks in relative circulation and the period with small values from 3 to 7 October. However, the agreement is not as good as with the wind components since FNL and NDR2 underestimate the relative circulation almost all days and ERA40 shows large overestimations on some days.

The detrained mass flux presented in Fig. 12 d shows small values of mass convergence into the EPIC domain in the layer 1000–850 hPa during almost all the P3 missions. No correlation with either wind component nor the relative circulation is evident from the figure. In general, analyses do not show a good correlation with observations and the largest differences are observed from 16 September to 6 October.

4. Conclusions

Two global reanalyses and the FNL analysis were studied in this paper to assess their validity in the East Pacific region. Observations from the EPIC2001 experiment and data from TAO moorings along

Please cite this article in press as: Marín, J.C., et al., Assessment of global numerical models in the East Pacific as evidenced from EPIC2001 project. Dyn. Atmos. Oceans (2008), doi:10.1016/j.dynatmoce.2008.10.001

95° W were used to accomplish the objectives of the study. The vertical structure and near-surface conditions of the atmosphere along 95° W and some dynamical aspects in the ITCZ constituted the basis against which to compare the different assimilated data.

All global analyses represent reasonably well the mean vertical wind profiles in the ABL and at all heights within the ITCZ at 95°W. However, relative large differences are shown in the ABL over the ITCZ due to the small wind values present as a consequence of the wind convergence over that region. The best agreement with observations is observed in the ABL, from the equator to 7°N, with absolute errors less than 1.6 ms^{-1}. All analyses represent poorly the wind components along 95° W in the 850–600 hPa layer south of the ITCZ. Over the tropical Pacific ABL, winds seem to behave in geostrophic balance (Raymond et al., 2006). For this reason, large differences in representing the wind field, particularly the zonal component, would result in large differences in the surface meridional pressure gradient that drives the meridional flow into the ITCZ, which has a key role in the development of deep convection.

Global analyses do not reproduce accurately the temperature profiles observed in the cold tongue region (near the equator). FNL shows the best agreement reproducing the θ_e lapse rates observed at all latitudes in the ABL and immediately above. However, θ_e lapse rates from analyses show a more unstable ABL at the equator and underestimate the inversion layer immediately above it. In general, all analyses overestimate the smallest observed saturation fraction values, while they underestimate the largest saturation fraction values along 95°W. FNL shows the best agreement with observations.

Surface pressure from C-130 in situ data agrees very well with MSLP from TAO buoys. All analyses show the observed surface pressure decrease from the equator to the ITCZ region. Reanalyses differ in less than 1 hPa from observations at all latitudes, and FNL shows absolute errors less than 2 hPa. NDR2 shows the best agreement among analyses, which maybe results in the least difference shown at representing the observed mean surface meridional wind variation with latitude. In general, near-surface zonal wind values are reasonably well reproduced from the equator to 7° N in all analyses but the v-component is much better represented at all latitudes. The largest discrepancies are observed in the ITCZ region due to the small wind values there.

Near-surface temperature in analyses shows a reasonable good agreement with observations. A closer agreement is shown with TAO observations than with dropsondes from the equator to 8°N. However, the agreement is better with dropsondes north of 8°N. The poorest representation of temperature in all analyses is observed at the equator, were absolute errors as large as 1.9 ° C are shown. The analysis of near-surface relative humidity shows small differences between all analyses and observations.

Bulk fluxes calculated from analyses show reasonably well the latitudinal variation of bulk surface fluxes calculated from observations along 95°W. The largest differences among bulk fluxes are shown from 2° N to 7° N where large air temperature-SST differences and strong surface winds are observed. All analyses overestimate the bulk wind stress calculated from observations at latitudes near the equator and underestimate it at latitudes within the ITCZ region.

All analyses seem to represent fairly well the transitions in the ITCZ zonal winds at 850 hPa as a result of the easterly wave passages over the region. However, NDR2 did not represent it at some times. The time evolution of the surface meridional wind is also represented fairly well by all analyses. Westerly periods in the ITCZ are associated with strong surface southerly winds, which result in enhanced convection and indicate an increase in the relative circulation in the region. In addition, easterlies coincide with a decrease in relative circulation, which could be related to the decrease in the convective activity over the region. The relative circulation and the detrained mass flux in the EPIC domain, averaged over the layer 1000-850 hPa, show large differences between analyses and observations. However, at some times a reasonable agreement with observations is observed by all or some of the analyses at all pressure levels. It is thought that differences with observations in those two variables are related with the different horizontal resolution of data, and thus the averaging region, and that observations were taken over a period of several hours but were compared with the single nearest time in analyses. The averaged wind field in the ITCZ is reasonably well reproduced by all global datasets, which could support their use in dynamical studies on the region. Unfortunately, the same cannot be said for the relative circulation and detrained mass flux.

In general, all analyses show large differences with observations in the region from the equator to 5°N. Mean vertical wind profiles in the layer 850–600 hPa, vertical θ_e profiles in the ABL, near-surface temperature at the equator, and surface fluxes from 2° N to 7° N present appreciable differences with

Please cite this article in press as: Marín, J.C., et al., Assessment of global numerical models in the East Pacific as evidenced from EPIC2001 project. Dyn. Atmos. Oceans (2008), doi:10.1016/j.dynatmoce.2008.10.001

observations in that region. This indicates that results from these global analyses must be used with caution between the equator and 5°N, where the largest differences with observations are shown. In spite of this, the best agreement in the wind field between datasets and observations is shown in the ABL over that region, where MSLP and near-surface temperature (except at the equator) show a reasonable agreement.

ERA40 seems to reproduce with more accuracy the mean ABL wind field characteristics observed in the East Pacific during the EPIC2001 experiment, compared with NCEP datasets. However, this is not always true with respect to the thermodynamic and near-surface analysis since FNL shows the best agreement reproducing the θ_e lapse rates observed at all latitudes in the ABL and immediately above, and representing the moisture content of the atmosphere. Furthermore, NDR2 represents much better the MSLP and near-surface meridional wind variation with latitude among datasets. In general, all analyses could be used to study mean conditions over the region, taking into account the above-mentioned limitations.

Acknowledgments

This work was carried out with the aid of a grant from the Inter-American Institute for Global Change Research (IAI) CRN II # 2048 which is supported by the US National Science Foundation (Grant GEO -0452325). This work was also aid by a scholarship from the Dirección General de Estudios de Posgrado, UNAM. ECMWF ERA-40 data used in this study have been obtained from the ECMWF data server at http://data.ecmwf.int/data/d/era40 daily. NCEP-DOE Reanalysis 2 data was provided by the NOAA/OAR/ESRL PSD, Boulder, Colorado, USA, from their Web site at http://www.cdc.noaa.gov/ and FNL data was obtained from the NCAR Web site http://www.dss.ucar.edu/datasets/ds083.2/data.

References

Abarca, S., 2005. Flujos turbulentos de Superficie sobre el Océano Pacífico Tropical Oriental. M.Sc. Thesis. Centro de Ciencias de la Atmósfera, UNAM.

Back, L.E., Bretherton, C.S., 2006. The relationship between wind speed and precipitation in the Pacific ITCZ. J. Climate 18, 4317–4328.

Bolton, D., 1980. The computation of equivalent potential temperature. Mon. Wea. Rev. 108, 1046–1053.

Bretherton, C.S., Peters, M.E., Back, L.E., 2004a. Relationships between water vapor path and precipitation over the tropical oceans. J. Climate 17, 1517–1528.

Bretherton, C.S., Uttal, T., Fairall, C.W., Yuter, S.E., Weller, R.A., Baumgardner, D., Comstock, K., Wood, R., Raga, G.B., 2004b. The Epic 2001 Stratocumulus Study. Bull. Am. Meteorol. Soc. 85, 967–977.

Brown, R.G., Zhang, C., 1997. Variability of midtropospheric moisture and its effect on cloud-top height distribution during TOGA COARE. J. Atmos. Sci. 54, 2760–2774.

Carr, M.T., Bretherton, C.S., 2001. Convective momentum transport over the tropical Pacific: budget estimates. J. Atmos. Sci. 58, 1673–1693.

Chelton, D.B., Esbensen, S.K., Schlax, M.G., Thum, N., Freilich, M.H., Wentz, F.J., Gentemann, C.L., McPhaden, M.J., Schopf, P.S., 2001. Observations of coupling between surface wind stress and sea surface temperature in the eastern tropical Pacific. J. Climate 14, 1479–1498.

De Szoeke, S., Bretherton, C.S., Bond, N.A., Cronin, M.F., Morley, B.M., 2005a. EPIC 95° W Observations of the eastern Pacific atmospheric boundary layer from the cold tongue to the ITCZ. J. Atmos. Sci. 62, 426–442.

De Szoeke, S., Bretherton, C.S., 2005b. Variability in the southerly flow into the eastern Pacific ITCZ. J. Atmos. Sci. 62, 4400–4411.

Fairall, C.W., Bradley, E.F., Hare, J.E., Grachev, A.A., Edson, J.B., 2003. Bulk parameterization of air–sea fluxes: updates and verification for the COARE algorithm. J. Climate 16, 571–591.

Kanamitsu, M., Ebisuzaki, W., Woollen, J., Yang, S-K., Hnilo, J.J., Fiorino, M., Potter, G.L., 2002. NCEP-DEO AMIP-II Reanalysis (R-2). Bull. Atmos. Please check the journal title of reference Kanamitsu et al. (2002).Meterol. Soc., 1631–1643.

Lindzen, R.S., Nigam, S., 1987. On the role of sea surface temperature gradients in forcing low-level winds and convergence in the tropics. J. Atmos. Sci. 44, 2418–2436.

McGauley, M., Zhang, C., Bond, N., 2004. Large-scale characteristics of the atmospheric boundary layer in the eastern Pacific cold tongue–ITCZ region. J. Climate 17, 3907–3920.

McPhaden, M.J., Busallacchi, A.J., Cheney, R., Donguy, J.-R., Gage, K.S., Halpern, D., Ji, M., Julian, P., Meyers, G., Mitchum, G.T., Niiler, P.P., Picaut, J., Reynolds, R.W., Smith, N., Takeuchi, K., 1998. The tropical ocean global atmosphere observing system: a decade of progress. J. Geophys. Res. 103 (C7), 14169–14240.

Nigam, S., Chung, C., Weaver, E., 2000. ENSO diabatic heating in ECMWF and NCEP-NCAR reanalyses, and NCAR CCM3 simulation. J. Climate 13, 3152–3171.

Petersen, W., Cifelli, R., Boccippio, D., Rutledge, S., Fairall, C., 2003. Convection and easterly wave structures observed in the eastern Pacific warm pool during EPIC-2001. J. Atmos. Sci. 60, 1754–1773.

Raymond, D.J., Raga, G.B., Bretherton, C.S., Molinari, J., López-Carrillo, C., Fuchs, Z., 2003. Convective forcing in the Intertropical Convergence Zone of the eastern Pacific. J. Atmos. Sci. 60, 2064–2082.

Please cite this article in press as: Marín, J.C., et al., Assessment of global numerical models in the East Pacific as evidenced from EPIC2001 project. Dyn. Atmos. Oceans (2008), doi:10.1016/j.dynatmoce.2008.10.001

Raymond, D.J., Esbensen, S.K., Paulson, C., Gregg, M., Bretherton, C.S., Petersen, W.A., Cifelli, R., Shay, L.K., Ohlmann, C., Zuidema, P., 2004. EPIC2001 and the coupled ocean–atmosphere system of the tropical East Pacific. Bull. Amer. Meteor. Soc. 85, 1341–1354.

Raymond, D., Zeng, X., 2005. Modeling tropical atmospheric convection in the context of the weak temperature gradient approximation. Quart. J. Roy. Meteorol. Soc. 131, 1301–1320.

Raymond, D.J., Bretherton, C.S., Molinari, J., 2006. Dynamics of the Intertropical Convergence Zone of the East Pacific. J. Atmos. Sci. 63, 582–597.

Romero-Centeno, R., Zavala-Hidalgo, J., Raga, G.B., 2007. Midsummer gap winds and low-level circulation over the Eastern Tropial Pacific. J. Climate 20, 3768–3784.

Stevens, B., Duan, J., McWilliams, J.C., Münnich, M., Neelin, J.D., 2002. Entrainment, Rayleigh friction, and boundary layer winds over the tropical Pacific. J. Climate 15, 30–44.

Uppala, S.M., Kallberg, P.W., Simmons, A.J., Andrae, U., Bechtold, V.D., Fiorino, M., Gibson, J.K., Haseler, J., Hernandez, A., Kelly, G.A., Li, X., Onogi, K., Saarinen, S., Sokka, N., Allan, R.P., Andersson, E., Arpe, K., Balmaseda, M.A., Beljaars, A.C.M., Van De Berg, L., Bidlot, J., Bormann, N., Caires, S., Chevallier, F., Dethof, A., Dragosavac, M., Fisher, M., Fuentes, M., Hagemann, S., Holm, E., Hoskins, B.J., Isaksen, L., Janssen, P.A.E.M., Jenne, R., McNally, A.P., Mahfouf, J.F., Morcrette, J.J., Rayner, N.A., Saunders, R.W., Simon, P., Sterl, A., Trenberth, K.E., Untch, A., Vasiljevic, D., Viterbo, P., Woollen, J., 2005. The ERA-40 Reanalysis. Quart. J. R. Meteorol. Soc. 131, 2961–3012.

Yin, B.F., Albrecht, B.A., 2000. Spatial variability of atmospheric boundary layer structure over the eastern equatorial Pacific. J. Climate 13, 1574–1592.

Zhang, C., McGauley, M., Bond, N.A., 2004. Shallow meridional circulation in the tropical eastern Pacific. J. Climate 17, 133–139.

Zuidema, P., Mapes, B., Lin, J., Fairall, C., Wick, G., 2006. The interaction of clouds and dry air in the eastern tropical Pacific. J. Climate 19, 4531–4544.

Please cite this article in press as: Marín, J.C., et al., Assessment of global numerical models in the East Pacific as evidenced from EPIC2001 project. Dyn. Atmos. Oceans (2008), doi:10.1016/j.dynatmoce.2008.10.001